GEOLOGY | THE GEOLOGICAL SOCIETY OF AMERICA®

https://doi.org/10.1130/G48132.1

Manuscript received 12 July 2020
Revised manuscript received 12 September 2020
Manuscript accepted 16 September 2020

Recycling of mercury from the atmosphere-ocean system into volcanic-arc–associated epithermal gold systems

Changzhou Deng[1], Guangyi Sun[2], Yimeng Rong[2], Ruiyang Sun[1], Deyou Sun[3], Bernd Lehmann[4] and Runsheng Yin[1]*

[1]State Key Laboratory of Ore Deposit Geochemistry, Institute of Geochemistry, Chinese Academy of Sciences, Guiyang 550081, China
[2]State Key Laboratory of Environmental Geochemistry, Institute of Geochemistry, Chinese Academy of Sciences, Guiyang 550081, China
[3]College of Earth Sciences, Jilin University, Changchun 130061, China
[4]Department of Mineral Resources, Technical University of Clausthal, Clausthal-Zellerfeld 38678, Germany

ABSTRACT

Photochemical processes generate mass-independent fractionation (MIF) of mercury (Hg) isotopes in the atmosphere-ocean system, and the subduction of marine sediments or hydrated oceanic crust may recycle the resultant Hg isotope signature into the volcanic-arc environment. This environment typically hosts epithermal gold deposits, which are characterized by a specific Hg-Sb-As metal association. We investigated the Hg isotopic composition of seven volcanic-arc–related epithermal gold deposits in northeast China and revisited the isotopic composition of Hg in hydrothermal ore deposits in circum-Pacific and Mediterranean volcanic arcs. The gold ore samples in northeast China mostly display positive Δ^{199}Hg values (0.11‰ ± 0.07‰, 1σ, *n* = 48) similar to those observed in the Pacific Rim (0.07‰ ± 0.09‰, 1σ, *n* = 182) and the Mediterranean Cenozoic volcanic belt (0.09‰ ± 0.08‰, 1σ, *n* = 9). Because Hg in marine sediments and seawater has positive Δ^{199}Hg, we infer that Hg-bearing epithermal deposits in active continental margin settings receive most Hg from recycled seawater in marine sediments, through the release of Hg by dehydration from the subducting oceanic slab. However, negative to near-zero Δ^{199}Hg values were observed in Hg-bearing deposits in the South China craton (–0.09‰ ± 0.05‰, 1σ, *n* = 105) and in the intraplate magmatic-hydrothermal Almadén Hg deposit in Spain (–0.02‰ ± 0.06‰, 1σ, *n* = 26), which are considered to relate to basement and mantle sources, respectively. Hg isotopes have the potential to trace lithospheric Hg cycling.

INTRODUCTION

Mercury (Hg) receives global concern due to its toxicity. The biogeochemical cycling of Hg in Earth's surface environment has attracted much interest; however, the cycling of Hg in the lithosphere remains poorly understood. Due to its chalcophile and volatile character, Hg is abundant in epithermal sulfide deposits, often in a shallow low-temperature environment as part of the larger porphyry-epithermal ore deposit spectrum. Ore deposits of this spectrum form in active continental margin settings (White and Hedenquist, 1995), where subduction of oceanic crust and concomitant release of Hg from the subducting oceanic slab may contribute to the typical Hg component in epithermal gold deposits.

Mercury isotopes may help to evaluate the amount of oceanic Hg in subduction-related hydrothermal deposits. With the discovery that Hg isotopes undergo both mass-dependent fractionation (MDF, expressed as δ^{202}Hg) and mass-independent fractionation (MIF, expressed as Δ^{199}Hg), Hg isotope geochemistry provides new and multidimensional information about the sources and fates of Hg in the environment (Blum et al., 2014). Hg-MDF is observed during various physical, chemical, and biological processes. However, Hg-MIF is primarily associated with photochemical processes (reviewed by Blum et al., 2014); therefore Hg-MIF signals can be a direct source tracer of Hg. Significant Hg-MIF signals are mainly found in Earth's surface environments (e.g., soil, water, sediment, atmosphere, and biological samples) and crustal materials (e.g., sedimentary rocks; Blum et al., 2014, and references therein), whereas mantle-derived Hg has no Hg-MIF (Δ^{199}Hg ~0; Sherman et al., 2009).

Hg-MIF with Δ^{199}Hg ranging from –0.30‰ to 0.36‰ has been observed in hydrothermal deposits (Fig. 1A; Smith et al., 2005, 2008; Yin et al., 2016, 2019; Xu et al., 2018; Fu et al., 2020; Pribil et al., 2020), indicating that Hg from surface reservoirs may be involved during Hg mineralization. To verify this speculation, we used Δ^{199}Hg as a potential proxy to study the source of Hg in seven subduction-related epithermal gold deposits in northeast China (Fig. 1B). Combined with previous results on the volcanic-arc–related Amiata Hg deposit in Italy, and in comparison to low-temperature Au-Sb-Pb-Zn deposits in South China and the intraplate magmatic-hydrothermal Almadén Hg deposit in Spain, we demonstrate that the subduction of ocean crust likely delivers a substantial amount of marine Hg to epithermal deposits in active continental margins.

GEOLOGICAL BACKGROUND

Seven Mesozoic calc-alkaline volcanoplutonic rock–related epithermal Au deposits (Sandaowanzi, Yongxin, Pangkaimen, Tuanjiegou, Fuqiang, Jinchang, and Sipingshan) were selected in northeast China (Fig. 1B), which is situated between the Siberia and North China cratons, at the intersection of the Paleozoic Central Asian orogenic belt and the Mesozoic–Cenozoic Pacific orogenic belt (Figs. 1C and 1D). The simplified tectonic evolution of northeast China is summarized in the Supplemental Material[1].

Both the Sandaowanzi and Yongxin deposits are characterized by Au-telluride mineralization occurring in the quartz vein and breccia systems. Gold orebodies in Tuanjiegou, Fuqiang,

*E-mail: yinrunsheng@mail.gyig.ac.cn

[1]Supplemental Material. Geological background, samples and methods, and analytical results for hydrothermal Au deposits in northeast China. Please visit https://doi.org/10.1130/GEOL.S.13076288 to access the supplemental material, and contact editing@geosociety.org with any questions.

CITATION: Deng, C., et al., 2020, Recycling of mercury from the atmosphere-ocean system into volcanic-arc–associated epithermal gold systems: Geology, v. 49, p. , https://doi.org/10.1130/G48132.1

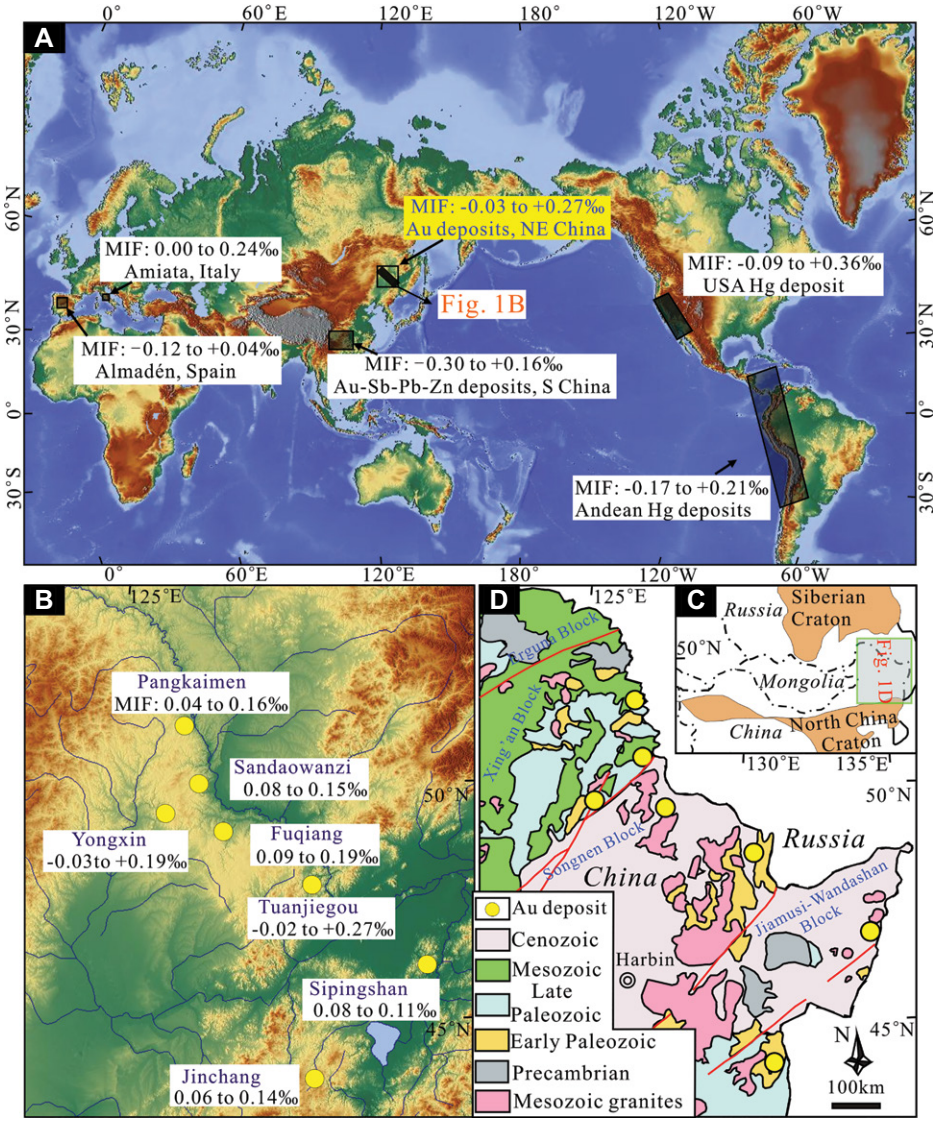

Figure 1. (A) Map showing hydrothermal deposits with Hg mass-independent fractionation (Hg-MIF) values. Data in the white squares are from previous studies: Hg deposits along the West Coast of the United States from Smith et al. (2005, 2008), Stetson et al. (2009), and Smith, (2010); Amiata Hg deposit, Italy, from Pribil et al. (2020); Almadén Hg deposit, Spain, from Gray et al. (2013); Andean Hg deposits from Cooke et al. (2013); Au-Sb-Pb-Zn deposits in South China from Xu et al. (2018), Yin et al. (2019), and Fu et al. (2020). (B) Enlarged map showing locations of studied Au deposits and Hg-MIF values. (C) Tectonic sketch map of the Central Asian orogenic belt (after Jahn, 2004). (D) Simplified geological map of eastern northeast China with seven gold deposits studied marked (after Xue, 2012).

and Pangkaimen occur as veined, brecciated, and lenticular bodies with gold mineralization dominated by gold-bearing pyrite-chalcedony and pyrite-calcite assemblages. The ores in the Jinchang mine include auriferous breccias, quartz-sulfide veins, and disseminated mineralization. The Sipingshan Au deposit is a hot-spring–type deposit. Its orebodies are hosted by chert, silicified breccias, and silicified rhyolites, with pyrite as the main sulfide mineral. Wall-rock alteration, including sericitization, silicification, carbonatization, pyritization, and chloritization, is developed in these Au deposits. Zircon U-Pb ages of the igneous host rocks and hydrothermal sericite Ar-Ar dating demonstrate that the Au deposits formed in the Early Cretaceous with ages ranging from 125 to 105 Ma (Xue, 2012). The S-Pb isotopic compositions show that the ore-forming components mainly originated from igneous source rocks with no or negligible significance of magmatic assimilation or fluids equilibrated with the sedimentary country rocks (Xue, 2012; Zhai et al., 2015). Fluid inclusion data indicate that mixing of meteoric and magmatic water triggered the precipitation of Au (Xue, 2012; Li et al., 2020).

SAMPLES AND ANALYTICAL METHODS

In total, 48 samples, including 7 volcanic wall rocks and 41 ores (7 of which were prepared for pyrite concentrates), were collected from the selected deposits (see the Supplemental Material). Total Hg concentration (THg) and Hg isotopic composition were analyzed at the Institute of Geochemistry, Chinese Academy of Sciences, Guiyang, China, following previous methods (see the Supplemental Material). Hg-MDF is expressed in δ^{202}Hg notation in units of ‰ referenced to the NIST-3133 Hg standard (analyzed before and after each sample):

$$\delta^{202}\mathrm{Hg}\ (‰) = [(^{202}\mathrm{Hg}/^{198}\mathrm{Hg}_{\mathrm{sample}})/(^{202}\mathrm{Hg}/^{198}\mathrm{Hg}_{\mathrm{standard}}) - 1] \times 1000. \quad (1)$$

Hg-MIF is reported in Δ notation, which describes the difference between the measured δ^{xxx}Hg value and the theoretically predicted δ^{xxx}Hg value, in units of ‰:

$$\Delta^{xxx}\mathrm{Hg} \approx \delta^{xxx}\mathrm{Hg} - \delta^{202}\mathrm{Hg} \times \beta, \quad (2)$$

where β is equal to 0.2520 for ^{199}Hg, 0.5024 for ^{200}Hg, and 0.7520 for ^{201}Hg (Blum and Bergquist, 2007).

Hg CONCENTRATION AND ISOTOPIC COMPOSITION

Hg concentrations and isotopic compositions of the samples are summarized in Text S2 (Table S1 in the Supplemental Material). THg concentration varied by orders of magnitude among pyrite (2.30–21.5 ppm), ore (0.033–7.64 ppm), and volcanic wall rocks (0.005–0.045 ppm). The δ^{202}Hg and Δ^{199}Hg values of the samples showed large ranges of –2.20‰ to 0.10‰ and –0.02‰ to 0.27‰, respectively, which are significant, given the 2σ analytical uncertainty of δ^{202}Hg (±0.1‰) and Δ^{199}Hg (±0.05‰). No clear differences in δ^{202}Hg and Δ^{199}Hg were observed among pyrite, ore, and wall-rock samples ($p > 0.05$, Student's t test). However, a negative correlation was observed between δ^{202}Hg and Δ^{199}Hg, and a positive correlation was observed between Δ^{201}Hg and Δ^{199}Hg (Fig. 2A).

Previous results on hydrothermal deposits of various types worldwide are summarized in Figure 2 for comparison. Large ranges of δ^{202}Hg (–2.52‰ to 1.99‰) and Δ^{199}Hg (–0.30‰ to 0.36‰), with a negative correlation between δ^{202}Hg and Δ^{199}Hg and a positive correlation between Δ^{201}Hg and Δ^{199}Hg, were observed in these reference deposits as well. According to Hg-MIF signals, the compiled data set (for data sources: see the caption of Fig. 1) can be divided into three groups: (1) Hydrothermal Hg deposits in active continental margin settings mainly show positive Δ^{199}Hg (e.g., Pacific Rim, mean = 0.07‰ ± 0.09‰, 1σ, n = 182; and Amiata, Italy, 0.09‰ ± 0.08‰, 1σ, n = 9; Fig. 1), similar to our results on gold deposits in northeast China (0.11‰ ± 0.07‰, 1σ, n = 48). (2) Hg-bearing hydrothermal deposits (e.g., Carlin-type Au deposits, hydrothermal base-metal and Sb deposits) in the South China craton mainly

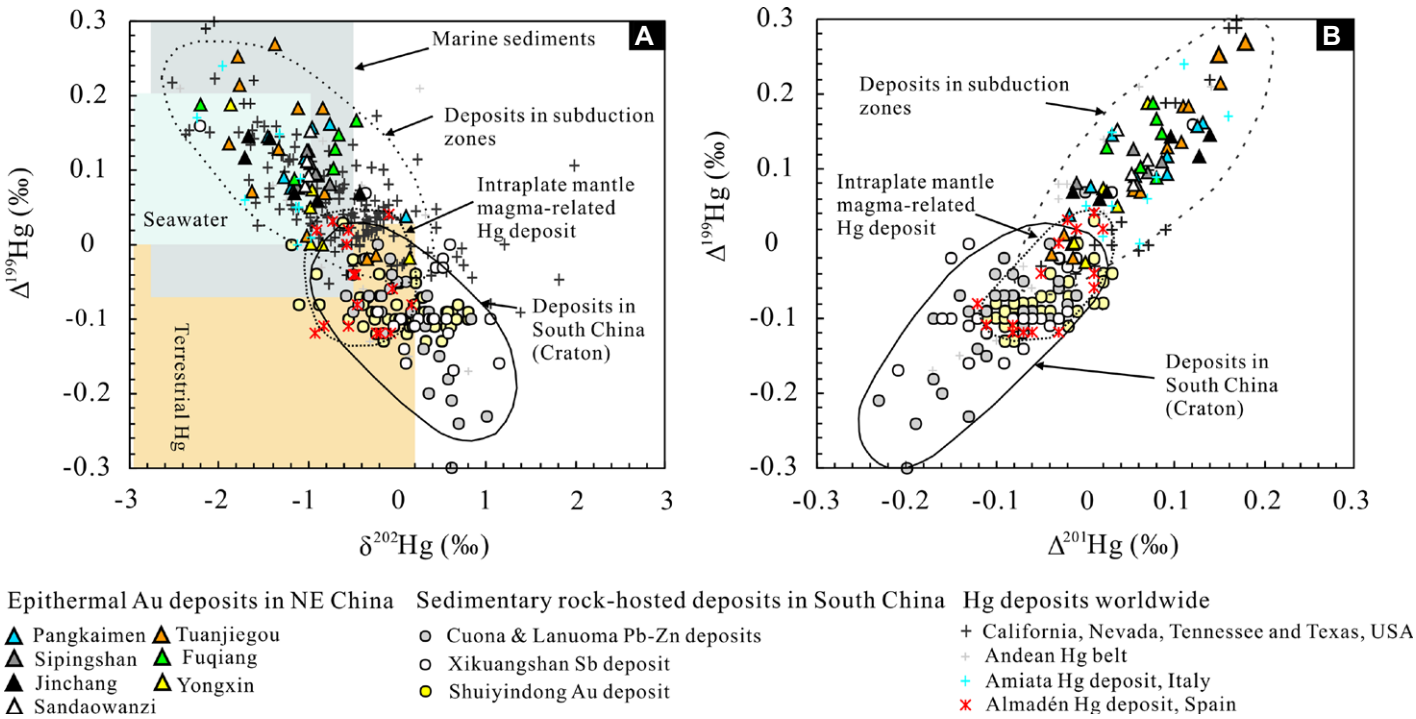

Figure 2. (A) Δ^{199}Hg versus δ^{202}Hg and (B) Δ^{199}Hg versus Δ^{201}Hg diagrams for studied Au deposits in northeast China and hydrothermal deposits worldwide. Data sources for deposits are as in Figure 1. For the subset of data points from Smith et al. (2005, 2008), Δ^{201}Hg values were plotted because mass ^{199}Hg was not measured, and the Δ^{199}Hg/Δ^{201}Hg ratio in these samples is expected to be close to 1.0 (Blum et al., 2014). Area of marine sediments is that defined by Yin et al. (2015) and Meng et al. (2019), terrestrial Hg is that defined by Blum et al. (2014, and references therein), and seawater is that defined by Štrok et al. (2015).

show negative Δ^{199}Hg (–0.09‰ ± 0.05‰, 1σ, n = 105; Fig. 1). These sediment-hosted deposits have no direct connection to volcanic-arc magmatism. (3) The Almadén Hg deposit in Spain shows near-zero Δ^{199}Hg (–0.02‰ ± 0.06‰, 1σ, n = 26; Fig. 1). This deposit was suggested to be sourced from intraplate mafic magma (Higueras et al., 2013).

MIF OF Hg ISOTOPES

The large variation of the Hg isotopic composition in epithermal gold deposits in northeast China (Fig. 2A) may be explained by the mixing of Hg sources with distinct isotopic signatures. Because various processes can trigger MDF (Blum et al., 2014), to avoid ambiguous interpretations, we will not discuss δ^{202}Hg further.

However, Hg-MIF mainly occurs during photochemical processes with little contribution from complex biogeochemical cycling, and therefore it provides clear constraints on Hg sources. As shown in Figure 2B, samples from hydrothermal deposits from northeast China and elsewhere show a Δ^{199}Hg/Δ^{201}Hg ratio of ~1.0, similar to that reported during aqueous Hg(II) photoreduction (Bergquist and Blum, 2007). Primordial Hg in mantle rocks is characterized by Δ^{199}Hg of ~0. However, once emitted to the surface environment, Hg(II) photoreduction in aquatic ecosystems can imprint the Hg-MIF signature, leading to negative Δ^{199}Hg values in the product Hg(0) and positive Δ^{199}Hg values in the residual Hg(II) pool (Bergquist and Blum, 2007). Terrestrial reservoirs (e.g., plants, soil, coal) are characterized by negative Δ^{199}Hg due to Hg(0) deposition, whereas aquatic reservoirs (e.g., rain and seawater) are characterized by positive Δ^{199}Hg due to Hg(II) deposition (Blum et al., 2014). In the ocean, coastal sediments commonly show negative Δ^{199}Hg values due to continental runoff, whereas marine sediments show positive Δ^{199}Hg values due to the scavenging of seawater Hg by particles (Yin et al., 2015; Meng et al., 2019). Mineralization processes are unlikely to induce Hg-MIF; therefore, the Hg-MIF observed in hydrothermal deposits indicates Hg sourced from Earth's surface reservoirs (Yin et al., 2016).

SUBDUCTION DELIVERS THE POSITIVE Hg-MIF SIGNATURE IN HYDROTHERMAL DEPOSITS NEAR ACTIVE CONTINENTAL MARGINS

The positive Δ^{199}Hg spectrum observed in the epithermal gold deposits in northeast China and Hg deposits in active continental margins elsewhere suggests a common phenomenon. There are two possible sources with positive Δ^{199}Hg: (1) meteoric water; and (2) fluid-rock interaction and devolatilization from sedimentary country rocks. Although meteoric water plays an important role in triggering the precipitation of ore minerals, its extremely low Hg concentrations (0.35–11 ng/L; Chen et al., 2012) rule out any significant contribution in the gold deposits. The northeast China strata consist mainly of late Paleozoic sandstone and siltstone, reflecting a coastal depositional environment, where sediments are mainly characterized by negative Δ^{199}Hg (Yin et al., 2014; Meng et al., 2019). S-Pb isotopic data from the epithermal Au deposits in northeast China indicate that the ore-forming components were likely derived from igneous rocks through fluid exsolution during crystallization instead of leaching of sedimentary country rocks (Xue, 2012). Combined with the absence of sedimentary rocks in most of the selected Au deposits, the contribution of Hg from sedimentary rocks can probably be precluded.

Considering that the epithermal and porphyry Au deposits commonly occur in subduction settings, an alternative cause of the positive Δ^{199}Hg in the epithermal gold deposits in northeast China could be the subduction of oceanic crust with marine sediments and seawater. The subduction zone environment plays an important role in energy and mass exchange between oceanic and continental plates (Tatsumi and Eggins, 1995; Zheng, 2019). Extensive hydrothermal activity has created large numbers of Hg and Hg-bearing deposits in active continental margin settings (Rytuba, 2003). The subduction process, with concomitant release of Hg and other volatile components from the descending oceanic plate (Fig. 3A), plays an important role in creating volcanic arcs and their geothermal/hydrothermal systems. The positive Δ^{199}Hg values in the ocean reservoir (marine

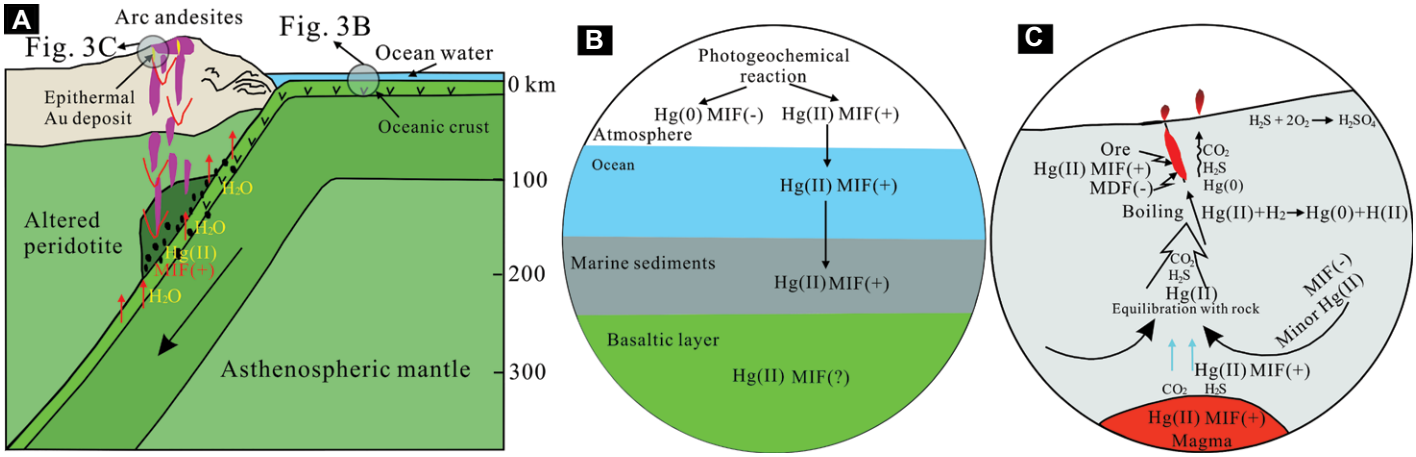

Figure 3. Proposed scenarios showing (A) subduction of the oceanic crust, which delivers positive mass-independent fractionation mercury (Hg-MIF) from the ocean reservoir to magmatic-hydrothermal deposits in active continental margins (modified after Zheng, 2019); (B) Hg-MIF signals in the ocean reservoir; and (C) hydrothermal processes during formation of epithermal Au deposits (after White and Hedenquist, 1995; Smith et al., 2005). MDF—mass-dependent fractionation.

sediments and seawater; Fig. 3B) would be inherited in the fluids released from the oceanic slab during plate dehydration. Aqueous fluids with marine Hg values could trigger the partial melting of the mantle wedge, and then they would be transported to the upper crust by mantle magma. Finally, Hg would be released into magmatic-hydrothermal fluids during crystallization and precipitated in the Au deposits when mixed with meteoric water (Fig. 3C). Figure 2A shows a broadly negative correlation trend between Δ^{199}Hg and δ^{202}Hg for hydrothermal deposits in active continental margins, suggesting mixing of two Hg source end members. One end member could be mantle Hg, which is likely characterized by Δ^{199}Hg of ~0‰ (Sherman et al., 2009). The other end member seems to be characterized by Δ^{199}Hg of ~0.3‰, which agrees well with previous results on marine sediments and seawater (Blum et al., 2014, and references therein; Štroket al., 2014; Ogrinc et al., 2019).

The distinct Δ^{199}Hg values observed in low-temperature deposits in the South China craton and the intraplate mantle magma–related Almadén Hg deposit in Spain suggest different sources of Hg from those in active continental margins. The low-temperature deposits in South China seem to have received most of their Hg from regional basement rocks, as these rocks are characterized by negative Δ^{199}Hg (Xu et al., 2018; Fu et al., 2020). The near-zero Δ^{199}Hg values observed in the Almadén Hg deposit are similar to those reported for mantle materials (Sherman et al., 2009), consistent with a previous study demonstrating that Hg was sourced from intraplate mafic magma (Higueras et al., 2013).

CONCLUSIONS AND IMPLICATIONS

We demonstrate that Hg-MIF is a common feature of hydrothermal ore deposits in active continental margins and also within cratons. Hg-MIF can serve as a robust tracer for the origin of Hg in hydrothermal deposits. For hydrothermal ore deposits at active continental margins, the positive Hg-MIF signals suggest that Hg was sourced from ocean reservoirs. Subduction of oceanic crust delivers positive Hg-MIF from marine sediments or seawater into the subduction zone, and this Hg is released from the subducting slab during dehydration to finally form epithermal deposits in active continental margins. For the low-temperature Au-Sb-Pb-Zn deposits in South China and the Almadén Hg deposit in Spain, local basement rock dehydration or fluid release from enriched mantle melts may play a more important role in contributing Hg to those hydrothermal deposits. Our study, thus, provides new insight into the lithospheric cycling of Hg.

ACKNOWLEDGMENTS

This work was supported by the National Natural Science Foundation of China (grants 41873047 and 41603020). We especially thank Chen Tang for help with field sampling, and editor Dennis Brown, and reviewers Stephen Grasby, Steve Kesler, and an anonymous reviewer for their helpful comments.

REFERENCES CITED

Bergquist, B.A., and Blum, J.D., 2007, Mass-dependent and -independent fractionation of Hg isotopes by photoreduction in aquatic systems: Science, v. 318, p. 417–420, https://doi.org/10.1126/science.1148050.

Blum, J.D., and Bergquist, B.A., 2007, Reporting of variations in the natural isotopic composition of mercury: Analytical and Bioanalytical Chemistry, v. 388, p. 353–359, https://doi.org/10.1007/s00216-007-1236-9.

Blum, J.D., Sherman, L.S., and Johnson, M.W., 2014, Mercury isotopes in earth and environmental sciences: Annual Review of Earth and Planetary Sciences, v. 42, p. 249–269, https://doi.org/10.1146/annurev-earth-050212-124107.

Chen, J.B., Hintelmann, H., Feng, X.B., and Dimock, B., 2012, Unusual fractionation of both odd and even mercury isotopes in precipitation from Peterborough, ON, Canada: Geochimica et Cosmochimica Acta, v. 90, p. 33–46, https://doi.org/10.1016/j.gca.2012.05.005.

Cooke, C.A., Hintelmann, H., Ague, J.J., Burger, R., Biester, H., Sachs, J.P., Burger, R., Biester, H., Sachs, J.P., and Engstrom, D.R., 2013, Use and legacy of mercury in the Andes: Environmental Science & Technology, v. 47, p. 4181–4188, https://doi.org/10.1021/es3048027.

Fu, S.L., Hu, R.Z., Yin, R.S., Yan, J., Mi, X.F., Song, Z.C., and Sullivan, N.A., 2020, Mercury and in situ sulfur isotopes as constraints on the metal and sulfur sources for the world's largest Sb deposit at Xikuangshan, southern China: Mineralium Deposita, v. 55, p. 1353–1364, https://doi.org/10.1007/s00126-019-00940-1.

Gray, J.E., Pribil, M.J., and Higueras, P.L., 2013, Mercury isotope fractionation during ore retorting in the Almadén mining district, Spain: Chemical Geology, v. 357, p. 150–157, https://doi.org/10.1016/j.chemgeo.2013.08.036.

Higueras, P., Oyarzun, R., Lillo, J., and Morata, D., 2013, Intraplate mafic magmatism, degasification, and deposition of mercury: The giant Almadén mercury deposit (Spain) revisited: Ore Geology Reviews, v. 51, p. 93–102, https://doi.org/10.1016/j.oregeorev.2012.12.004.

Jahn, B.M., 2004, The Central Asian orogenic belt and growth of the continental crust in the Phanerozoic, *in* Malpas, J., et al., eds., Aspects of the Tectonic Evolution of China: Geological Society [London] Special Publication 226, p. 73–100, https://doi.org/10.1144/GSL.SP.2004.226.01.05.

Li, C.L., Li, L., Yuan, M.W., Alam, M., Li, S.R., Santosh, M., Deng, C.Z., Liu, H., and Xu, G.Z., 2020, Study on pyrite thermoelectricity, ore-forming fluids and H-O-Rb-Sr isotopes of the Yongxin gold deposit, Central Asian orogenic belt: Implications for ore genesis and exploration: Ore Geology Reviews, v. 121, p. 103568, https://doi.org/10.1016/j.oregeorev.2020.103568.

Meng, M., Sun, R.Y., Liu, H.W., Yu, B., Yin, Y.G., Hu, L.G., Shi, J.B., and Jiang, G.B., 2019, An integrated model for input and migration of mercury in Chinese coastal sediments: Environmental Science & Technology, v. 53, p. 2460–2471, https://doi.org/10.1021/acs.est.8b06329.

Ogrinc, N., Hintelmann, H., Kotnik, J., Horvat, M., and Pirrone, N., 2019, Sea as revealed by mercury stable isotopes: Scientific Reports, v. 9, p. 11626, https://doi.org/10.1038/s41598-019-48061-z.

Pribil, M.J., Rimondi, V., Costagliola, P., Lattanzi, P., and Rutherford, D.L., 2020, Assessing mercury distribution using isotopic fractionation of mercury processes and sources adjacent to and downstream of a legacy mine district in Tuscany, Italy: Applied Geochemistry, v. 117, p. 104600, https://doi.org/10.1016/j.apgeochem.2020.104600.

Rytuba, J.J., 2003, Mercury from mineral deposits and potential environmental impact: Environmental Geology, v. 43, p. 326–338, https://doi.org/10.1007/s00254-002-0629-5.

Sherman, L.S., Blum, J.D., Nordstrom, D.K., McCleskey, R.B., Barkay, T., and Vetriani, C., 2009, Mercury isotopic composition of hydrothermal systems in the Yellowstone Plateau volcanic field and Guaymas Basin sea-floor rift: Earth and Planetary Science Letters, v. 279, p. 86–96, https://doi.org/10.1016/j.epsl.2008.12.032.

Smith, C.N., 2010, Isotopic Geochemistry of Mercury in Active and Fossil Hydrothermal Systems [Ph.D. thesis]: Ann Arbor, Michigan, Department of Geological Sciences, University of Michigan, 164 p.

Smith, C.N., Kesler, S.E., Klaue, B., and Blum, J.D., 2005, Mercury isotope fractionation in fossil hydrothermal systems: Geology, v. 33, p. 825–828, https://doi.org/10.1130/G21863.1.

Smith, C.N., Kesler, S.E., Blum, J.D., and Rytuba, J.J., 2008, Isotope geochemistry of mercury in source rocks, mineral deposits and spring deposits of the California Coast Ranges, USA: Earth and Planetary Science Letters, v. 269, p. 399–407, https://doi.org/10.1016/j.epsl.2008.02.029.

Stetson, S.J., Gray, J.E., Wanty, R.B., and Macalady, D.L., 2009, Isotopic variability of mercury in ore, mine-waste calcine, and leachates of mine-waste calcine from areas mined for mercury: Environmental Science & Technology, v. 43, p. 7331–7336, https://doi.org/10.1021/es9006993.

Štrok, M., Hintelmann, H., and Dimock, B., 2014, Development of pre-concentration procedure for the determination of Hg isotope ratios in seawater samples: Analytica Chimica Acta, v. 851, p. 57–63, https://doi.org/10.1016/j.aca.2014.09.005.

Štrok, M., Baya, P.A., and Hintelmann, H., 2015, The mercury isotope composition of Arctic coastal seawater: Comptes Rendus Geoscience, v. 347, p. 368–376, https://doi.org/10.1016/j.crte.2015.04.001.

Tatsumi, Y., and Eggins, S., 1995, Subduction Zone Magmatism: Oxford, UK, Blackwell Science, 211 p.

White, N.C., and Hedenquist, J.W., 1995, Epithermal gold deposits: Styles, characteristics and exploration: SEG Newsletter, v. 23, p. 1, 9–13.

Xu, C.X., Yin, R.S., Peng, J.T., Hurley, J.P., Lepak, R.F., Gao, J.F., Feng, X.B., Hu, R.Z., and Bi, X.W., 2018, Mercury isotope constraints on the source for sediment-hosted lead-zinc deposits in the Changdu area, southwestern China: Mineralium Deposita, v. 53, p. 339–352, https://doi.org/10.1007/s00126-017-0743-7.

Xue, M.X., 2012, Metallogenesis of Endogenic Gold Deposits in Heilongjiang Province [Ph.D. thesis]: Changchun, China, Jilin University, 162 p.

Yin, R.S., Feng, X.B., and Chen, J.B., 2014, Mercury stable isotopic compositions in coals from major coal producing fields in China and their geochemical and environment implications: Environmental Science & Technology, v. 48, p. 5565–5574, https://doi.org/10.1021/es500322n.

Yin, R.S., Feng, X.B., Chen, B., Zhang, J., Wang, W., and Li, X., 2015, Identifying the sources and processes of mercury in subtropical estuarine and ocean sediments using Hg isotopic composition: Environmental Science & Technology, v. 49, p. 1347–1355, https://doi.org/10.1021/es504070y.

Yin, R.S., Feng, X.B., Hurley, J.P., Krabbenhoft, D.P., Lepak, R.F., Hu, R.Z., Zhang, Q., Li, Z., and Bi, X.W., 2016, Mercury isotopes as proxies to identify sources and environmental impacts of mercury in sphalerites: Scientific Reports, v. 6, p. 18686, https://doi.org/10.1038/srep18686.

Yin, R.S., Deng, C.Z., Lehmann, B., Sun, G.Y., Lepak, R.F., Hurley, J.P., Zhao, C.H., Xu, G.W., Tan, Q.P., Xie, G.Z., and Hu, R.Z., 2019, Magmatic-hydrothermal origin of mercury in Carlin-style and epithermal gold deposits in China: Evidence from mercury stable isotopes: ACS Earth & Space Chemistry, v. 3, p. 1631–1639, https://doi.org/10.1021/acsearthspacechem.9b00111.

Zhai, D.G., Liu, J.J., Ripley, E.M., and Wang, J.P., 2015, Geochronological and He-Ar-S isotopic constraints on the origin of the Sandaowanzi gold-telluride deposit, northeastern China: Lithos, v. 212–215, p. 338–352, https://doi.org/10.1016/j.lithos.2014.11.017.

Zheng, Y.F., 2019, Subduction zone geochemistry: Geoscience Frontiers, v. 10, p. 1223–1254, https://doi.org/10.1016/j.gsf.2019.02.003.

Printed in USA